The Cryosphere Discuss., 6, 2115–2160, 2012
www.the-cryosphere-discuss.net/6/2115/2012/
doi:10.5194/tcd-6-2115-2012

The Cryosphere Discussions

Climatic drivers of seasonal glacier mass balances: an analysis of 6 decades at Glacier de Sarennes (French Alps)

E. Thibert[1], N. Eckert[1], and C. Vincent[2]

[1]IRSTEA, UR ETGR Erosion Torrentielle Neige et Avalanches, BP 76, 2 rue de la papeterie, Saint Martin d'Hères, France
[2]CNRS/UJF-Grenoble 1, LGGE Laboratoire de Glaciologie et Géophysique de l'Environnement, BP 96, 54 rue Molières, Saint Martin d'Hères, France

Received: 7 May 2012 – Accepted: 4 June 2012 – Published: 14 June 2012

Correspondence to: E. Thibert (emmanuel.thibert@irstea.fr)

Published by Copernicus Publications on behalf of the European Geosciences Union.

Abstract

Refined temporal signals are extracted from a glacier winter and summer mass balance series recorded at Glacier de Sarennes (French Alps) using variance decomposition. They are related to local and synoptic meteorological data in terms of interannual variability and structured trends. The winter balance has increased by +23 % since 1976 due to more precipitation in early and late winter. The summer balance has decreased since 1982 due to a 43 % increase in snow and ice melt. A 24-day lengthening of the ablation period – mainly due to longer ice ablation – is the main component in the overall increase in ablation. In addition, the last 25 yr have seen increases in ablation rates of 14 and 10 % for snow and ice respectively. A simple degree-day analysis can account for both the snow/ice melt rate rise and the lengthening of the ablation period as a function of higher air temperatures. From the same analysis, the equilibrium line altitude of this 45° North latitude south-facing glacier has sensitivity to temperature of $+93\,\mathrm{m\,^{\circ}C^{-1}}$ around its mean elevation of 3100 m a.s.l. over 6 decades. The sensitivity of summer balance to temperature is $-0.62\,\mathrm{m\,w.e.\,yr^{-1}\,^{\circ}C^{-1}}$ for a typical 125-day long ablation season. Finally, the time structure of winter and summer mass balance terms are connected to NAO anomalies. Best correlations are obtained with winter NAO anomalies. However, they strongly depend on how the NAO signal is smoothed, so that the link between mass-balance seasonal terms and NAO signal remains tenuous and hard to interpret.

1 Introduction

Mountain glaciers are recognized as excellent indicators of climate change over the last few centuries (Oerlemans and Fortuin, 1992; Haeberli, 1995; Vincent, 2002; IPCC, 2007). Glacier length fluctuations are the oldest and most numerous measurements (Oerlemans et al., 1998) but they provide a climatic signal that is delayed, filtered (high frequency cutting) and dependent on glacier dynamics (Johannesson et al., 1989). In contrast, surface mass balance is a more direct climatic signal. From a thermodynamic point of view, a glacier is an open system which exchanges mass and energy with its environment. As most alpine glaciers are temperate (with the temperature at the melting point), energy exchanges (radiation and sensible heat) result mainly in a loss of mass through melting, while ice condensation and sublimation are negligible in the mass budget of alpine glaciers (Sicart et al., 2008). Winter precipitation recorded in the accumulation term accounts for almost all the overall system mass input (Braithwaite, 1981; Oerlemans, 1993, 2001; Vincent and Vallon, 1997; Vincent, 2002). Summer melt variability is mainly dependent on short-wave radiation which correlates well with air temperature (Sicart et al., 2008; Pellicciotti et al., 2008). Glacier mass-balance can therefore be used to assess climate warming on a regional scale (Vincent et al., 2004; Huss and Bauder, 2009).

Nevertheless, inferring the climatic signal from a glacier mass balance series is not easy. The glacier-wide mass-balance is a convolution between climate evolution and glacier geometry changes in response to climate fluctuations (Elsberg et al., 2001; Ohmura et al., 2007; Harrison et al., 2009). As an illustration of the glacier topography feed-back, when a glacier tongue retreats, ablation areas of strong negative budget are removed from the average balance, tending to make it less negative. Conversely, a lowering of the glacier surface tends to force the surface energy balance in relation with altitudinal gradient of the mass balance. Moreover, as pointed out by Harrison et al. (2009) and Huss et al. (2012), the combination of both these effects can have different results on glacier-average balance from one glacier to another.

To overcome these artifacts, Elsberg et al. (2001) proposed to relate mass balance to a constant geometry correcting for surface and altitude changes. They successfully made such an adjustment for South Cascade Glacier and Rasmussen (2009) extended this correction to the two seasonal components of the balance. An alternative is to directly use surface mass balances measured at an individual location and use a single or a few sites (Huss and Bauder, 2009; Vincent et al., 2004). When point-to-point balances are significantly correlated, this local analysis has a glacier-wide significance (Rasmussen, 2004; Rasmussen and Andreassen, 2005; Thibert and Vincent, 2009).

A difficulty is that long data series are affected some years by missing values of winter or summer balances at some locations. Missing values in the summer balance term are often estimated with temperature index models (Huss and Bauder, 2009) but, at this stage, a method that does not use meteorological data should be used to extract a self-sufficient unbiased temporal signal and interpret its link with climatic drivers. An interesting option that fits this requirement is analysis of variance (ANOVA) that separates the overall annual effect from spatial variability at the glacier surface (Lliboutry, 1974). Missing values are reconstructed using information from the other measurements at the glacier surface without any assumption concerning meteorological conditions and their relationship to mass balance seasonal components.

Here, we interpret the 6-decade long seasonal balance recorded on Sarennes glacier (French Alps) by applying the expansion of Lliboutry's analysis of variance model proposed by Eckert et al. (2011) to extract the winter and summer terms from the recorded winter and annual point measurements. Being performed in a hierarchical context, this approach has the advantage of separating the structured low-frequency temporal signal that affects the whole glacier from random fluctuations in the balance between years and between sites. The refined temporal signals obtained include annual glacier-wide fluctuations and underlying time trends and change points. They are then related to independent series of data on precipitation and temperature, and potential connections to larger-scale atmospheric patterns are inferred from North Atlantic Oscillation anomalies. For both local and synoptic covariates, correlations are investigated for annual values and low-frequency patterns (i.e. trends). After a presentation of the site and of the method used to treat the data (Sect. 2), this analysis is conducted and discussed for the winter (Sect. 3) and summer (Sect. 4) mass-balance components.

2 Site, data and method

2.1 Sarennes mass balance data

Sarennes is a small south-facing glacier (0.4 km^2 in 2003) with a small altitude range of 150 m, located in the Grande Rousses range (45°07 N; 6°07 E; French Alps). Since 1949, systematic winter and summer mass balance measurements have been carried out. This makes the Sarennes data series the second longest series of winter and summer mass balances in the Alps after Claridenfirn (Müller and Kappenberger, 1991). On four to five sites (Fig. 1), two different measurement methods are used for accumulation and ablation measurements: (a) cores are first drilled to measure winter mass balances from snow layering (stratigraphy) and density measurements, (b) annual mass balances are determined from stakes inserted in ice. The summer mass balance is the difference between these two balance terms. Sarennes data have been checked using a geodetic method (Thibert et al., 2008) and have been shown to be consistent. Measurements are repeated 6 to 7 times through the ablation period, not on fixed dates but based on use of the stratigraphic method to determine the maximum balance at the end of winter and minimum at the end of the ablation period (Cogley et al., 2010). Therefore the numerous observations on the glacier make it possible to decipher changes in the rate and duration of ablation in summer balance variations. Here we analyse the 1949–2007 data table (59 yr × 5 sites = 295 data) among which 27 values are missing due to measurements that were not carried out (Thibert and Vincent, 2009).

2.2 Extraction of the seasonal components using variance decomposition

Extending the precursor work of Lliboutry (1974), different models to extract temporal patterns related to climatic forcing are presented and compared by Eckert et al. (2011). Here, we briefly describe the model that was found to be most suitable for Sarennes.

The temporal β_t signal is first extracted from a linear variance model according to:

$$b_{i,t} = \alpha_i + \beta_t \tag{1}$$

where α_i is the mean balance recorded at location i over the period of record. Hence, β_t is the annual deviation from the mean (centred balance). Based on previous work on streamflow (Perrault et al., 2000a, b) and snow avalanche runout elevation modelling (Eckert et al., 2010), β_t is taken as centred on a linear trend with constant c_j and annual rate d_j, σ_j being the standard deviation of the regression residuals, and τ the year preceding a possible rupture in trend and/or variance in each component of the balance (subscript j = [1, 2] before/after the change point):

$$\beta_t = N(c_j + d_j t; \sigma_j^2) \tag{2}$$

Equation (1) is applied to both measured winter and annual balances (b^w, b^a). The third component, summer balance b^s, is available from $b^s = b^a - b^w$ ($b^s < 0$). The correlation between the different variables is explicitly taken into account. Equation (2) is applied to the two winter and summer seasonal components instead of to the actually observed couple, allowing two change points in annual balance. Estimation is performed within a Bayesian framework using simulation-based methods for parameter estimation (Brooks, 1998) with evaluation of missing data (Tanner, 1996). As detailed in Eckert et al. (2011), the glacier-wide balance B_t (annual, winter or summer terms) only differs from β_t by a constant $\langle B \rangle$ which represents the glacier-wide mean balance over the whole period of record (1949–2007). Year-to-year variations of each mass balance seasonal terms can be therefore indifferently analyzed through β_t or B_t time series. This can be summarized by the following equations:

$$B_t^a = \beta_t^a + \langle B^a \rangle \text{ with } \langle B^a \rangle = -0.97\,\text{m w.e. yr}^{-1}, \tag{3}$$

$$B_t^w = \beta_t^w + \langle B^w \rangle \text{ with } \langle B^w \rangle = 1.69\,\text{m w.e. yr}^{-1}, \tag{4}$$

$$B_t^s = \beta_t^s + \langle B^s \rangle \text{ with } \langle B^s \rangle = -2.66\,\text{m w.e. yr}^{-1}, \quad (5)$$

where upper case letters refer to glacier-wide variables and the superscripts "a", "w", and "s" denote the annual, winter and summer terms, respectively. Signals extracted from such variance decomposition are plotted in Fig. 2.

From the analysis of these extracted time signals (Eckert et al., 2011), two marked change points are identified in winter and summer balances in 1976 and 1982, respectively, leading to a relative complex pattern in the annual mass balance signal with a short high regime period between 1976 and 1982 (Fig. 2a). The winter balance extracted from the analysis of variance is plotted in Fig. 2b. The change point identified and the corresponding sub-periods of different means and trends are given in Table 1. The change point in winter mass balance series is a very sharp change point in mean and trends just after 1976. The shift in winter precipitation after 1976 is $+0.66\,\text{m w.e. yr}^{-1}$ separating 2 periods of 1.48 and $1.88\,\text{m w.e. yr}^{-1}$ average accumulation with slightly negative trends in both periods.

The summer balance extracted from the analysis of variance is plotted in Fig. 2c. A change point in mean and variance is identified in 1982 but this one is much smoother than the 1976 winter balance change point. The corresponding periods of different means and trends are given in Table 2. The shift in summer balances in 1982 is $-0.96\,\text{m w.e. yr}^{-1}$ separating 2 periods of -2.26 and $-3.22\,\text{m w.e. yr}^{-1}$ averages.

Regarding correlations between extracted times series, the annual balance is mainly dependent on the summer balance with a correlation coefficient, hereafter denoted as r, of 0.89 (Table 2). The winter balance has a lesser effect with a correlation of 0.53. There is almost no correlation between winter and summer balances. Trends and change points account for 20–30 % of the variance of the different components of the balance, the rest being made-up of random interannual fluctuations. With respect to how trends are related to each other over the 6 decades, 83 % of the trends in the annual balance are related to the summer balance trends and there is almost no correlation between trends for the winter balance and the annual balance (Table 3).

2.3 Local meteorological variables

To infer potential drivers, we relate the extracted annual and low-frequency signals to annual and low-frequency signals in meteorological data of different scale relevance. In the vicinity of Sarennes glacier, an automatic weather station operating at 3000 m a.s.l. since 2004 records 30 min averages of air temperatures and relative humidity as well as wind speed and direction. To cover the entire mass-balance record period, daily temperatures measured at the meteorological station (Météo-France) in Lyon (200 m a.s.l.) are available. Located 120 km from Sarennes in the Rhone valley, the Lyon meteorological series can reasonably be used as temperature fluctuations are well correlated over large areas (Böhm et al., 2001). More specifically, Lyon summer temperatures correlate well with other meteorological stations closer to Sarennes but with shorter records (Vincent and Vallon, 1997). Over the common recording period, mean daily temperatures at the glacier automatic weather station correlate well with Lyon ($r = 0.85$; Fig. 3) especially between April and October ($r = 0.89$). The observed vertical lapse rate during the ablation period is 6.25 °C km^{-1}, just below the free-troposphere wet adiabatic vertical gradient of 6.5 °C km^{-1}. It drops to 4.9 °C km^{-1}in winter with a poor correlation ($r = 0.44$) between both weather stations. Considering these seasonal gradients to be constant along the mass balance record is supported by results of the 44 year-reanalysis of climate in the French Alps by (Durand et al., 2009a). Lyon temperatures (May to October annual means) are plotted in Fig. 4a over the 1949–2007 period. Analysis with a change point model similar to the one used for Sarennes highlights a gradual change in the middle of the 1970's (1974 ± 4 yr) followed by a strong and continuous increase (+1.32 °C) since 1982. Increases were greatest in August and May (+1.85 and +1.66 °C) and smallest in September (+0.58 °C). In winter months, the temperature has risen by about 1 °C. This main low-frequency pattern in summer temperatures is consistent with the results of a broad range of studies which show marked warming at high elevations since the middle of the 1970's, notably in the Alpine space (e.g. Beniston et al., 1997).

To relate precipitation on the glacier to the valley station, the nearest (6 km), long (since 1907) daily precipitation record is the meteorological station (Météo France) located at Besse en Oisans at an elevation of 1400 m a.s.l. Besse precipitations correlate poorly with Lyon but very well ($r = 0.97$) with Bourg d'Oisans 12 km away (Vincent and Vallon, 1997). Analysing the series with a change point model identifies a marked change point in 1976 with a strong shift separating two periods with a decreasing trend (Fig. 4b). This sharp breakpoint in winter precipitation is more regional than the summer temperature signal: it is significant for snowfalls and weather series in the northern French Alps (Durand et al., 2009a, b) but is not obvious at the larger scale of the entire European Alps (Quadrelli et al., 2001).

2.4 Synoptic meteorological variables

Although it is clear that regional climate drives the changes in the different seasonal mass balance terms, how they are controlled by larger-scale synoptic variables remains a more open question. A major difficulty is that it is hard to find among the several synoptic indexes available the ones that accurately summarise synoptic fluctuations and best correlate with glacier fluctuations. In the North Atlantic and Alpine space, most commonly studied data are NAO anomalies which are known to have a great influence on winter climate (e.g. Quadrelli et al., 2001). For this study, we used the classical monthly standardised series from Jones et al. (1997) complemented by Osborn (2006) for recent years. Three different cumulated anomalies have been considered: December to February (DJF, 3 months), November to March (NDJFBM, 6 months), and October to September (annual, 12 months).

Smoothing NAO anomalies is a recognised way of detecting similar patterns (i.e. low frequency trends) in local series and NAO data because, at the annual scale, NAO series are highly variable which compromises correlation. Another argument in favour of smoothing is that seasonal synoptic patterns can influence local climate for longer than they actually last (van Loon and Williams, 1976). NAO anomalies smoothed over several years have therefore been intensively used in Switzerland (Beniston, 1997, 2005;

Beniston and Jungo, 2002; Scherrer and Appenzeller, 2006) to discuss and explain recent changes in weather patterns and snow pack characteristics at high altitudes. For the French Alpine area space, smoothed NAO anomalies have been used by Durand et al. (2009a, b) in a similar way and by Six et al. (2001) to analyse several glacier mass balance data including Sarennes, but over a much shorter time period (1966–1998). Here, having sixty years of data on the three components of mass balance as well as their underlying trends, more significant correlations can be investigated as well as how the different components respond to synoptic forcing, both for the annual values and low-frequency signals.

However, the different NAO series cannot be statistically analysed in the same way as the Sarennes data and local covariates. Indeed, they show two change points in the underlying long term trend, around 1970 and 1990 respectively, rather than a single breakpoint separating two linear trends. This is clear for DJF anomalies after smoothing of the data with an 11-yr moving average filter to separate interannual variability from the structured signal. Furthermore, a 5-yr moving average filter hallmarks the well known 7–10 yr periodicity of the NAO signal (Fig. 4c) which is far from obvious in Sarennes series.

Considering the correlation as a function of the level of smoothing shows the frequencies at which seasonal mass balance fluctuations correlate most closely with the NAO signal. Different filters and time windows have been investigated. Figure 5 presents detailed results for DJF NAO anomalies processed with the retained triangular filters (i.e. weighted moving averages with weights decreasing linearly). It confirms that it is not at the annual scale that the different mass balance components are best correlated with the NAO signal. Very low correlations between annual anomalies and the different mass balance components slowly increase with the NAO filtering window size. Maximum correlation is reached with filtering windows of between 5 and 15 yr, depending on which variable is being considered, i.e. mean frequencies with respect to the duration of the whole investigated period. Correlations are, for all variables, systematically higher in absolute values and more significant between low-frequency patterns provided by

Eq. (2) and smoothed NAO signals than between the annual variables themselves, and smoothed NAO signals. This result shows the advantages and limitations of comparing smoothed data and/or trends instead of the variables themselves. It points up similarly structured changes, e.g. similar changes in local variables and large scale patterns. Hence, in some ways, it is better to compare smoothed values for local variables with synoptic variables smoothed over several years than "rough" local annual values with synoptic variables smoothed over several years. However, the problem of comparing two smoothed signals is that, for large smoothing windows, significant correlations will nearly always be obtained as soon as the data are not entirely random. To limit this bias, in the rest of the paper, we use the lowest level of smoothing necessary to obtain optimum correlation with Sarennes data, i.e. a 7-yr time window (current value ±3 yr) for the various NAO anomalies considered.

3 Winter mass balance

3.1 Link with local covariates

For each year of the period of record, the glacier-wide winter balance B_t^w obtained from the analysis of variance has been plotted against precipitations recorded at Besse weather station over the same period (end of ablation season year $n-1$, measurement date winter balance year n; Fig. 6). Only days of solid precipitation with temperatures below 1 °C are concerned, rain being assumed to run off the glacier and not to contribute to mass balance when the temperature is higher. Temperatures on the glacier are calculated from the Lyon weather station with a 4.9 °C km^{-1} mean altitudinal gradient for the winter season. Varying by 1–2 °C, the rain-snow divide does not significantly change the results.

Figures 2b and 4b show the 1976 change point in both Sarennes winter balance and Besse precipitations. Furthermore, Besse and Sarennes winter data correlate well ($r = 0.81$; Table 2). The same correlation is observed in trends provided by Eq. (2) in

Table 3. Coherence in trends and change point between Besse and Sarennes indicate a similar behaviour in terms of time-structured interannual patterns.

With a fixed date calculation (October–May), correlation drops from $r = 0.81$ to $r = 0.73$, close to the 0.75 value reported by Vincent and Vallon (1997) over the shorter period 1949–1994. Examining monthly precipitations at Besse in more detail shows that precipitation changes since 1976 are mainly due to increases in early winter (October) and late winter (March, April and May). On the other hand, no trend or rupture is observed in precipitation in the middle of winter. Analyzing Lyon temperatures reveals that winter (October–May) temperatures increased by 1.09 °C, with the highest increases recorded in May, October and March (+1.67 °C, +1.48 °C and +1.23 °C, respectively). Warming in November to February is only +0.8 °C. Increased precipitation observed at Sarennes since 1976 could therefore be related to milder temperature conditions in winter, particularly in early and late winter. More precipitation associated with higher temperature and decreasing snow cover in early summer is documented by (Durand et al., 2009a) for the French Alps, and even at the larger scale of mid latitudes (McCabe and Wolock, 2010).

Regarding precipitation and accumulation, Fig. 6 shows the ratio between winter mass balance at Sarennes and Besse winter precipitation. The ratio of 2.5 confirms the large difference between the amount of valley precipitation and winter accumulation at high elevation. Considering that this ratio may differ considerably from one glacier to another, this value is close to that of 2–3 reported between Besse and Saint-Sorlin glacier (5 km from Sarennes) for the same altitude range (Vincent, 2002). Ratios in the range 2.3–2.6 are also indicated for Glacier Blanc (Rabatel et al., 2008) with a comparable altitude difference (1600 m) between the glacier and the closest downhill weather station. This ratio corresponds to a mean altitudinal gradient of annual precipitation of 840 mm $(1000\,\mathrm{m})^{-1}$ which is 4 times higher than large-scale values of 200 mm $(1000\,\mathrm{m})^{-1}$ reported by (Durand et al., 2009a) for south and central Alps. This indicates that specific accumulation processes at the glacier scale supplement the classical orographic effect. A possible explanation already reported by (Vincent, 2002) is that wind

TCD
6, 2115–2160, 2012

drifts on surrounding nonglacial slopes and avalanches may capture snow over a larger area than the glacier itself. This indicates that the classical orographic gradient cannot be used to calculate winter accumulation at the scale of a high altitude englacial basin.

3.2 Link to NAO anomalies

There is almost no correlation between winter balance and NAO anomalies (Table 2), either for 3 month, 6 month or annual values. Results are very similar for Besse precipitations. This is reasonable since Besse correlates well with the Sarennes winter balance. These results are consistent with observations by Durand et al. (2009b) indicating a relatively surprising absence of correlation between winter NAO anomalies and snow cover data in the French Alps. This would suggest that winter balance at Sarennes is very weakly connected to the synoptic signal summarised in the NAO index. This strengthens the statement of a regional significance of the predominant temporal pattern in Sarennes winter balance and local high altitude precipitations (strong breakpoint in 1976). Indeed, if it is reported on other glaciers in the French Alps (Vincent, 2002), no specific trend or rupture is reported in glacier winter balances in the central and eastern Swiss Alps like Silvretta and Claridern glaciers (Müller and Kappenberger, 1991; Vincent et al., 2004; Huss and Bauder, 2009). Closer to Sarennes, only Aletsch glacier (Valis region) shows a synchronous change point in winter balance around 1974–1976 (Huss and Bauder, 2009), but this one is less sharp than observed for the French glaciers.

Our approach that extracts the structured trend in the various components of the Sarennes data and covariates also makes it possible to compare trends in precipitations in Besse and accumulation at Sarennes provided by Eq. (2) with the retained 7-yr smoothed NAO anomalies (Table 3). They are significantly correlated (Fig. 7a) with the relevant signal concentrated in the DJF series for which the correlation is the highest. The positive sign of the correlation is nevertheless surprising, since one would intuitively expect high snow accumulations to be associated with negative NAO anomalies. With respect to the limitation when it comes to comparing smoothed signals as highlighted in Sect. 2.4, this result must be interpreted with care since correlation is not equivalent to causality. Here, the trend in accumulation is mostly downward over the study period as a whole but with a strong shift around 1982. In contrast, the DFJ NAO anomaly decreased up to 1970 and again after 1990, i.e. over about two thirds of the studied period. The positive correlation between low-frequency patterns in accumulation and NAO anomalies may therefore represent nothing more than the predominance of negative trends in both time series and it does not necessarily imply that long-term changes in NAO anomalies really control long-term changes in winter balance in Sarennes.

4 Summer balance

Regarding snow and ice melt jointly, ablation has increased by 1.1 m w.e. yr^{-1} (+43 %) since 1982 (Table 4). This is due to both longer and more intense ablation. The duration of snow and ice ablation rose from 115 to 139 days (+24 days i.e. +19 %) between the 2 periods 1949–1982 and 1983–2007. Ablation starts 13 days earlier in spring (May) and continues for 11 days longer in autumn (October). In parallel, ablation rates rose by 0.44 cm w.e. day^{-1} (+22 %) over the last 25 yr of the record. Therefore the rise is due to both intensification (53 %) and longer ablation (47 %). However, analysing how snow and ice contribute separately to these ablation changes yields to more nuanced figures as discussed in the following Sects. 4.1 and 4.2.

4.1 Snow ablation

Distinction can be made between the rates and durations of snow and ice ablation by virtue of very extensive mass balance observations made during the melting season which make it possible to establish the snow-to-ice transition date within a few days at each measurement location. However, such an analysis requires considering point mass balance recorded at a single stake rather than an average for the overall glacier.

TCD
6, 2115–2160, 2012

As explained by (Thibert and Vincent, 2009) because the centred summer balance, β_t^s, is the common annual response at all measurement points, choosing the location that holds most of the information is choosing the one that correlates the best with the centred summer balance β_t^s, or identically, with the glacier-wide summer balance B_t^s (Sect. 2.2). We therefore select stake 4 which correlates best with β_t^s and explains the main part of the variance ($r = 0.97$) of the centred summer balance (Fig. 8).

Between the two periods highlighted by the variance decomposition model, snow ablation increased from 1.42 m w.e. yr^{-1} to 1.70 m w.e. yr^{-1} at stake no. 4 (Table 5). Its duration did not change between the 2 periods (mean 86 days). Ablation duration at stake 4 for snow is shown in Fig. 9. Snow ablation both starts and ends 13 days, earlier. The 0.28 m w.e. yr^{-1} snow ablation rise since the 80's is therefore exclusively due to intensification. Snow ablation rates have indeed risen from 1.77 cm w.e. day^{-1} before 1982 to 2.04 cm w.e. day^{-1} since. Therefore 25 % of the snow and ice ablation increase observed since 1982 is due to snow ablation intensification and not to an increase in snow ablation duration. As a consequence, because of earlier and higher snow melt, the date when the balance equals zero has therefore come forward by an average of 13 days from the 31 to the 17 August. Of course this analysis is limited for years with negative budget, ice ablation tends to occur therefore earlier after 1982 as analysed hereafter in Sect. 4.2. In accordance with our observations at Sarennes, shorter snow cover duration is particularly well documented at lower altitudes in the French Alps over 1958–2007 (Durand et al., 2009b). Note that the present results for snow ablation rate changes differ slightly from those calculated for Sarennes by (Vincent et al., 2004). This is due to a shorter period of record (1954–2002) in that previous paper. Moreover, for comparison with Claridenfirn Glacier, the 1st June was taken as a conventional fixed date for the beginning of the ablation season for the 2 glaciers.

With respect to temperature, a lot of studies have reported strong correlations with snow or ice ablation (e.g. Sicart et al., 2008 and references therein). Considering summer centred balances at Sarennes measured throughout the ablation season, mean temperatures recorded at Lyon correlate well ($r = -0.76$; Table 2). This correlation rises to −0.94 when considering trends over the 6 decades of record (Table 3). Such high correlations establish the empirical basis of well known positive degree-day (PDD) models relating melt to positive temperature sums (Hock, 1999, 2003). Considering measurements performed at stake 4 alone, Fig. 10 shows ablation during the snow ablation periods as a function of the cumulated positive temperatures calculated for the glacier from Lyon data with the vertical lapse rate of 6.25 °C km^{-1} identified in Sect. 2 under summer conditions. Using the numerous ablation measurements (a total of 253) performed each year during the ablation season, we identify a sensitivity of 0.41 cm w.e. °C^{-1} day^{-1} for snow ablation, with a strong correlation of $r = 0.89$. Our result is close the values of 0.38 cm w.e. °C^{-1} day^{-1} reported by Vallon and Vincent (1997) for Sarennes over a shorter timeframe, and 0.4 cm w.e. °C^{-1} day^{-1} for the Saint-Sorlin glacier located 3 km from Sarennes (Vincent, 2002). This result is unchanged if the analysis is performed separately on the two periods identified by the analysis of variance, indicating stable sensitivity to temperature for snow melting over the 6 decades of record. Figure 11 shows that this snow sensitivity coefficient, despite being somewhat variable (0.41 ± 0.08 cm w.e. °C^{-1} day^{-1}), is rather stable along the 6 decades of record at Sarennes. Therefore we do not identify at Sarennes a decreasing trend in snow ablation sensitivity as reported by Huss et al. (2009) since the 60's, and resulting from a detailed analysis of long ablation time series on 3 glaciers in the Swiss Alps.

As plotted in Fig. 4a, the Lyon temperature series shows a smooth, relatively continuous change point centred in the mid 1970's with a mean temperature shift of nearly +1 °C since 1974 for May to October. Because of the difficulty of segmenting the series into two clear sub-periods, we have adopted for the following analysis the 2 sub-periods identified for the summer balance with the break point occurring in 1982. Consequently, two curves have been plotted in Fig. 12 reporting raw and Gaussian smoothed mean daily temperatures above 0 °C at Sarennes (PDD) calculated from the Lyon data for the 2 periods 1949–1982 and 1983–2007. Figure 12 illustrates two main effects of warming during the ablation season:

1. Earlier snow ablation since 1983 with the number of days with mean positive temperatures increasing from 119 to 142 since 1983: these 23 additional days are very close to the 24 additional ablation days measured at stake 4, and show a similar distribution with 15 additional days above zero in May associated with ablation starting 13 days earlier.

2. Higher snow ablation rates due to higher temperatures: using the snow sensitivity of 0.41 cm w.e. $^{\circ}C^{-1}$ day^{-1} identified above, an additional snow ablation of 0.23 m w.e. is predicted since 1982 using the 2 temperature curves of Fig. 12, taking into account the change in the winter balance. This is in very good agreement with 0.28 m w.e. additional snow ablation measured at stake 4 (Table 5). Higher winter balances since 1976 have therefore been balanced by higher snow melt rates in relation to higher temperatures, resulting in almost constant snow ablation durations.

The preceding analysis can be used to quantify the sensitivity of Equilibrium-Line Altitude (ELA) to temperature. Over the 6 decades of record, the mean winter accumulation on the glacier is $\langle B^{w} \rangle = 1.69$ m w.e. yr^{-1}, with a very low spatial (altitudinal) dependence (Eckert et al., 2011). Using the snow ablation sensitivity of 0.41 cm w.e. $^{\circ}C^{-1}$ day^{-1}, this requires a degree-day amount of 412 °C day cumulated over the whole ablation season. Using a vertical lapse rate of 6.25 °C km^{-1} and Lyon temperatures, the mean altitude satisfying such a cumulated PDD condition is 3100 m. This altitude represents the mean ELA over 6 decades for this 45° N latitude south aspect Alpine glacier. Enhancing the mean temperature of 1 °C would increase the PDD sum of 138 °C day over the ablation season, yielding to a 0.57 m w.e. additional snow melt. Using a mass balance gradient with altitude in the range 0.7–0.8 m w.e. yr^{-1} (100 m)$^{-1}$ (Haeberli and Hoelzle, 1993), this will give an ELA sensitivity of 70–80 m $^{\circ}C^{-1}$. This is in agreement with Oerlemans (2001) for Alpine glaciers and a little higher than the value predicted by Vincent (2002) inferred from an analogous empirical PDD analysis on four glaciers in the French Alps. However, lengthening of

TCD
6, 2115–2160, 2012

the ablation season was not accounted for in this last study which probably underestimates the sensitivity by 10 %. Moreover, both of these PDD results are strongly dependent on the adopted vertical lapse rate (Caidong and Sorteberg, 2010). Our ELA sensitivity is well below the range of 120–160 m °C^{-1} reported by Oerlemans and Hoogendoorn (1989), Vallinga and Van de Wal (1998), Greene et al. (1999), Maish (2000), Gerbaux et al., (2005), Zemp and others, (2007). On the one hand, higher sensitivity can be explained by smaller mass balance gradient like that of 0.58 w.e. yr^{-1} (100 m)$^{-1}$ as reported by Gerbaux et al. (2005) which would result in a sensitivity of 98 m °C^{-1}. Measurements from the 5 stakes at Sarennes also suggest a lower gradient of 0.61 m w.e. yr^{-1} (100 m)$^{-1}$ between 2800 and 3000 m a.s.l. that would result in 93 m °C^{-1}. On the other hand, lower sensitivity could be related to feedback due to precipitation, cloud long wave radiation. Such effects are convoluted in the PDD regression while treated separately in model approaches. Furthermore, the vertical gradient of mass balance should not be a constant if climate is changing (Oerlemans and Hoogendoorn, 1989; Gerbaux et al., 2005).

A complementary result of this analysis is that a precipitation change of +34 % should compensate a temperature increase of +1 °C, assuming a linear response. This corresponds to an absolute change of +0.57 m w.e. yr^{-1} which is in agreement with the result of +0.5 m w.e. (=+28 %) reported by Gerbaux et al. (2005) on Saint-Sorlin glacier (5 km from Sarennes) using a physically based energy mass-balance model. Our result is also in agreement with the +25–30 % range for precipitation change given by Vincent (2002) based on field observations on four others glaciers in the northern French Alps.

4.2 Ice ablation

Considering all years of the record (including years with and without ice ablation), ice ablation has on average increased by 0.83 m w.e. yr^{-1} since 1983. Therefore 75 % of the ablation increase since 1982 (+1.1 m w.e. yr^{-1}) is explained by ice ablation alone. However, among the 59 yr of recorded mass balances, only 17 are positive mass balance years with solely snow ablation and 13 (76 %) of these occurred before 1982. Considering exclusively the negative-balance years over six decades of record, and again considering the 1949–1982 and 1983–2007 periods, ice ablation measured at stake 4 has increased by 0.73 m w.e. yr^{-1} from 1.07 m w.e. yr^{-1} to 1.80 m w.e. yr^{-1} (Table 5). Both ice ablation duration and ice ablation rates explain this shift. The ablation season has lengthened by 24 days and longer-lasting ice ablation explains all the increase in the ablation period since 1982 with the snow ablation period essentially remaining constant. Ice ablation lasted 29 days before 1982 and 53 days since, beginning 13 days earlier and ending 11 later (Fig. 9). Above and beyond its duration, ice ablation has also intensified: ablation rates increased by 0.25 cm w.e. day^{-1} (nearly 10 %) since 1982 and by between 2.50 cm w.e. day^{-1} and 2.75 cm w.e. day^{-1} since. The main part (87 %) of the rise in ice ablation is thus due to the extension of the ablation period and only 13 % due to melt intensification.

Analyzing ice ablation as function of positive degree-day calculated from Lyon data, Fig. 10 reports 144 measurements performed along the ice ablation period over the 6 decades of record, indicating a sensitivity of 0.68 cm w.e. $^{\circ}C^{-1}$ day^{-1} for ice ablation with a good correlation (r = 0.93). Again this sensitivity is consistent with that reported for Sarennes by Vincent and Vallon (1997) (0.62 cm w.e. $^{\circ}C^{-1}$ day^{-1}) between 1949 and 1994. This result is also in the range given by Laumann and Reeh (1993) for glaciers in Norway and Hock (1999) in Sweden. As reported for snow, we do not see any specific trend or time structure in the ice sensitivity over the 6 decades at Sarennes (Fig. 11).

Again, the effect of temperature rise on ice ablation rates and duration can be explained by the degree-day analysis of Fig. 12:

1. The autumn 11-day lengthening of the ice ablation season observed after 1982 from direct measurements is well explained by the number of additional days with mean positive temperatures in September–October at Sarennes (10 days as calculated on the basis of Lyon data). The 13-day earlier ice melt in August results also in higher melt rates, independently of the temperature rise, because average mid-August daily temperatures exceed those of September by 1.6 °C.

2. Higher ice ablation due to higher and longer-lasting positive temperature is also quantitatively explained. Using the snow sensitivity of 0.68 cm w.e. $^{\circ}C^{-1}$ day^{-1} identified above, an additional ice ablation of 0.79 m w.e. is predicted since 1983 using the 2 temperature curves of Fig. 12. This is in good agreement with 0.73 m w.e. additional ice ablation measured at stake 4 since 1982 (Table 5).

The sensitivity of ablation to temperature variations over the whole summer period can be deduced from our snow and ice ablation analysis over the last 6 decades. For this, the degree-day factor has been multiplied by the number of days when temperatures are positive. With a mean ablation period of 125 days, including 86 days of snow ablation and 39 days of ice ablation, we use a mean daily sensitivity of 0.49 cm w.e. $^{\circ}C^{-1}$ day^{-1}. This yields an ablation sensitivity of 0.62 m w.e. $^{\circ}C^{-1}$ at 3000 m. As sensitivity of ablation decreases with elevation (Vallon et al., 1998; Braithwaite and Zhang, 2000; Vincent, 2002), a similar analysis at stake 2, 83 m lower in altitude (Fig. 1), gives 0.64 m w.e. $^{\circ}C^{-1}$ at 2917 m, taking into account the fact that ablation lasts 10 days longer at this stake. Altitude range being small at Sarennes (150 m), it is difficult to retrieve a reliable estimate of the altitudinal dependence of the sensitivity, even taking into account data from other stakes. However, this result is within the range of 0.8 to 1.3 m w.e. $^{\circ}C^{-1}$ (1000 m)$^{-1}$ from Vallon et al. (1998) and Braithwaite and Zhang (2000), respectively.

Summing up, 75 % of ablation variations since the last 25 yr of the record are explained by the increased ice ablation in the summer balance component of the mass balance. This is mainly driven by the 24-day lengthening of the ablation period in late summer-early autumn and, to a lesser extent, by higher snow and ice ablation rates over the whole ablation period. The lengthening of the ablation period accounts therefore for 65 % of the ablation increase observed during the summer season. 35 % is related to higher ablation rates in which snow and ice account for 25 % and 10 %, respectively. Temperature – which exhibits common variance – can be used as an explicative variable: monthly temperatures between May and October have indeed increased by +1.32 °C, and those in September to October by +1.2 °C.

TCD
6, 2115–2160, 2012

4.3 Link with NAO anomalies

Summer balance at Sarennes is significantly negatively correlated with NAO anomalies and similar results are observed with Lyon temperature, as expected form the high correlation between summer balance and temperatures (Table 2). Again, these correlations are even stronger for trends than for the variables themselves (Table 3). More interestingly, it appears that correlations are much better with winter NAO series than with annual NAO anomalies and that the relevant signal is, as for winter balance, concentrated in the DJF series. Accordingly, Hurrell (1995) argues that NAO anomalies are not well defined over summer months due to a flatter pressure field. Indeed, correlations with the annual NAO signal, even smoothed, are not significant, and considering cumulative anomalies from November to April (which better represents the duration of winter conditions at high altitude) leads to correlations weaker than the DJF anomaly (Tables 2 and 3).

The physical explanation proposed by Beniston and Jungo (2002) for the positive correlation between NAO winter anomalies and high altitude summer temperatures (and therefore summer ablation) in the Alpine space is that positive winter anomalies are associated with high pressure blocking events in the Alps, inducing vertical atmospheric circulation, decreasing cloudiness, and thus persistent warming. Such blocking events have been frequently documented in recent years.

Since winter balance and DJF NAO anomalies are very weakly correlated, this positive correlation between summer balance and DJF NAO anomalies leads to a slightly negative correlation between winter NAO anomalies and Sarennes annual mass balance (Table 2) as has already been pointed out by (Six et al., 2001). This negative correlation is only statistically significant for smoothed signals (Fig. 7b, c and Table 3). This is compatible with the weak anti-correlation between NAO forcing and the mass balances of western European Alps glaciers inferred at a much larger spatial scale by (Marzeion and Nasje, 2012). It also suggests that the dependence of the interannual variability of the Sarennes mass balance on the synoptic signal summarised in the NAO

TCD
6, 2115–2160, 2012

is much weaker than reported by Huss et al. (2010) between reconstructed mass balances of 100 Swiss glaciers and sea surface temperatures in the North Atlantic Ocean (Atlantic Multidecadal Oscillation). This is reasonable as temperature is a larger-scale relevant variable. Temperature signals are well correlated over large areas (Böhm et al., 2001) and temperature correlates highly with summer and annual balances.

5 Conclusions

The winter and summer mass balances recorded at Glacier de Sarennes since 1949 have been subjected to an analysis of variance to identify changes in mean, trends and variance. The refined, extracted time-structured signals have been related to large (NAO) and glacier-scale forcing drivers in terms of annual fluctuations, change points and low-frequency trends.

Winter accumulation at the high altitude of Glacier de Sarennes is closely related to valley precipitations with about 65 % of common variance. Nevertheless the ratio between accumulation and precipitation recorded in valley weather stations is up to 2.5 for an altitude difference of 1500 m, which represents an average altitudinal gradient of 840 mm $(1000\text{ m})^{-1}$ of annual precipitation. This is 4 times the value expected from large-scale altitudinal orographic gradients which identify specific accumulation processes depending on basin topography. Regarding the temporal evolution of the winter balance, the sudden winter balance shift identified in 1976 is well documented in the western Alps. This is related to higher precipitations occurring in early and late winter months and could be associated with milder winters over the last 30 yr, especially in late winter.

With respect to summer balance, a change point is detected in 1982 and 2 explanatory processes underlie the very large increase of 1.1 m w.e. yr^{-1} in ablation: changes in both ablation duration and ablation rate. Lengthening explains around 65 % of the ablation rise with the ablation period tending to start 13 days earlier in spring and to end 11 days later in autumn. Snow ablation duration is mostly constant over 6 decades so prolongation of the ablation season is due to a 24-day lengthening of the ice ablation period. An increase in ablation rates also contributes to the summer balance change with similar shifts for snow and ice (0.25–0.27 cm w.e. day^{-1}). These changes in ablation rate contribute to a lesser extent (35 %) to the summer balance increase observed over the last 25 yr of the record.

From a single temperature analysis based on a simple degree day model, more than 80 % of summer balance variations can be explained by the atmospheric temperature rise since the early 80's, explaining quantitatively both ablation lengthening and intensification. From the direct measurements performed at Sarennes, snow and ice ablation sensitivity to temperature coefficients are stable over the 6 decades of record and no specific trend or time structure is detected in snow ablation sensitivity to temperature as reported by (Huss et al., 2009) in an analysis of long time series for 3 glaciers in the Swiss Alps.

The mean ELA of this 45° North latitude south-facing glacier was 3100 m a.s.l. between 1949 and 2007. Around this mean position, the sensitivity of the equilibrium line altitude to temperature change is about 93 m °C^{-1} although this is highly dependent on the adopted altitudinal dependence of mass balance which is +0.61 m w.e. yr^{-1} (100 m)$^{-1}$ at Sarennes. For the sensitivity of the summer balance to temperature, a value of −0.62 m w.e. yr^{-1} °C^{-1} can be derived by assuming a 125-day ablation period at 3000 m a.s.l. as observed over the last 6 decades.

The breakpoint and the linear trends indicated by the Sarennes observations correspond well to those observed in local climate covariates. They are not disconnected from large-scale patterns, e.g. they are consistent with the general context of warming since the middle of the 1970's. However, correlations between the different seasonal components of the balance and NAO anomalies have been found to be weak and hard to interpret. Significant correlations only emerge for December to February NAO anomalies, even for summer balance. Furthermore, the NAO signal has to be smoothed over several years to obtain significant correlations. This can generate artefacts and leads to somewhat surprising results such as the positive correlation between the trend in winter balance and DJF NAO anomalies. Hence, this study suggests that climatic control of interannual variability in the Sarennes' mass balance by the synoptic signal summarised in the NAO index is rather weak, and corresponds to the influence of blocking events in winter or spring on summer balance. There is therefore still much work to be done to link Sarennes data with different synoptic variables, e.g. direct pressure measurements instead of differences at the scale of the Northern Atlantic space and/or temperatures anomalies such as the AMO used by Huss et al. (2010).

Acknowledgements. The authors are grateful to the numerous people that have permitted the constitution of Sarennes's exceptional data series, especially L. de Crécy and F. Valla. Thank to their efforts, data collection has been, despite limited funds, nearly exhaustive during 60 yr. The last years of the record were funded by GLACIOCLIM Observatoire de Recherche en Environnement (ORE), Programme d'Observation des Glaciers (POG) and Observatoire des Sciences de l'Univers de Grenoble (OSUG, Institut des Sciences de l'Univers (INSU)). We thank also Météo-France for providing meteorological data.

References

Beniston, M.: Variations of snow depth and duration in the Swiss Alps over the last 50 years: links to changes in large-scale climatic forcing, Climatic Change, 36, 281–300, 1997.

Beniston, M.: Mountain Climates and Climatic Change: An Overview of Processes Focusing on the European Alps, Pure Appl. Geophys., 162, 1587–1606, 2005.

Beniston, M. and Jungo, P.: Shifts in the distributions of pressure, temperature and moisture and changes in the typical weather patterns in the Alpine region in response to the behavior of the North Atlantic Oscillation, Theor. Appl. Climatol., 71, 29–42, 2002.

Beniston, M., Diaz, H. F., and Bradley, R. S.: Climatic change at high elevation sites: an overview, Climatic Change, 36, 233–251, 1997

Braithwaite, R. J.: On glacier energy balance, ablation and air temperature, J. Glaciol., 27, 381–391, 1981.

Braithwaite, R. J. and Zhang, Y.: Sensitivity of mass balance of five Swiss glaciers to temperature changes assessed by tuning a degree-day model, J. Glaciol., 46, 7–14, 2000.

TCD

6, 2115–2160, 2012

An analysis of 6 decades at Glacier de Sarennes

E. Thibert et al.

Brooks, S. P.: Markov Chain Monte Carlo Method and its application, The Statistician, 47, 69–100, 1998.
Cogley, J. G., Hock, R., Rasmussen, L. A., Arendt, A. A., Bauder, A., Braithwaite, R. J., Jansson, P., Kaser, G., Möller, M., Nicholson, L., and Zemp, M.: Glossary of Glacier Mass Balance and Related Terms, IHP-VII Technical Documents in Hydrology No. 86, IACS Contribution No. 2, UNESCO-IHP, Paris, 2010.
Durand, Y., Laternser, M., Giraud, G., Etchevers, P., Lesaffre, B., and Mérindol, L.: Reanalysis of 44 year of climate in the French Alps (1958–2002): methodology, model validation, climatology, and trends for air temperature and precipitation, J. Appl. Meteorol. Climatol., 48, 429–449, 2009a.
Durand, Y., Laternser, M., Giraud, G., Etchevers, P., Mérindol, L., and Lesaffre, B.: Reanalysis of 47 Years of Climate in the French Alps (1958–2005): Climatology and Trends for Snow Cover, J. Appl. Meteorol. Climatol., 48, 2487–2512, 2009b.
Eckert, N., Baya, H., and Deschâtres, M.: Assessing the response of snow avalanche runout altitudes to climate fluctuations using hierarchical modelling: application to 61 winters of data in France, J. Climate, 23, 3157–3180, 2010.
Eckert, N., Baya, H., Thibert, E., and Vincent, C.: Extracting the temporal signal from a winter and summer mass-balance series: application to a six-decade record at Glacier de Sarennes, French Alps, J. Glaciol., 57, 134–150, 2011.
Elsberg, D. H., Harrison, W. D., Echelmeyer, K. A., and Krimmel, R. M.: Quantifying the effect of climate and surface change on glacier mass balance, J. Glaciol., 47, 649–658, 2001.
Gerbaux, M., Genthon, C., Etchevers, P., Vincent, C., and Dedieu, J. P.: Surface mass balance of glaciers in the French Alps: distributed modelling and sensitivity to climate change, J. Glaciol., 51, 561–572, 2005.
Greene, A., Broecker, W. S., and Rind, D.: Swiss glacier recession since the Little Ice Age: reconciliation with climate records, Geophys. Res. Lett., 26, 1909–1911, 1999.
Haeberli, W.: Glacier fluctuations and climate change detection, Geogr. Fis. Din. Quat., 18, 191–199, 1995.
Haeberli, W. and Hoelzle, M. (Compilers): Fluctuations of Glaciers, vol. VI, UNESCO, Paris, 1985–1990, 1993.
Harrison, W. D., Cox, L. H., Hock, R., March, R. S., and Petit, E. C.: Implications for the health of a glacier from comparison of conventional and reference-surface balances, Ann. Glaciol., 50, 25–30, 2009.

Hock, R.: A distributed temperature-index ice- and snowmelt model including potential direct solar radiation, J. Glaciol., 45, 101–11, 1999.
Hock, R.: Temperature index melt modelling in mountain areas, J. Hydrol., 282, 104–115, doi:10.1016/S0022-1694(03)00257-9, 2003.
Hurrell, J. W.: Decadal trends in the North Atlantic Oscillation: Temperatures and precipitation, Science, 269, 676–679, 1995.
Huss, M. and Bauder, A.: Twentieth-century climate change inferred from long-term point observations of seasonal mass balance, Ann. Glaciol., 50, 207–214, 2009.
Huss, M., Funk, M., and Ohmura, A.: Strong Alpine glacier melt in the 1940s due to enhanced solar radiation, Geophys. Res. Lett., 36, L23501, doi:10.1029/2009GL040789, 2009.
Huss, M., Hock, R., Bauder, A., and Funk, M.: 100-year mass changes in the Swiss Alps linked to the Atlantic Multidecadal Oscillation, Geophys. Res. Lett., 37, L10501, doi:10.1029/2010GL042616, 2010.
Huss, M., Hock, R., Bauder, A., and Funk, M.: Conventional versus reference-surface mass balance, J. Glaciol., 58, 278–286, 2012.
Intergovernmental Panel on Climate Change (IPCC): Climate Change 2007, in: Contribution of the Working Group I to the Third Assessment Report of the Intergovernmental Panel on Climate Change, 996 pp., edited by: Solomon, S., Qin, D., Manning, M., Chen, Z., Marquis, M., Averyt, K. B., Tignor, M., and Miller, H. L., Cambridge Univ. Press., New York, 2007.
Johannesson, T., Raymond, C., and Waddington, E.: Time-scale for adjustment of glaciers to changes in mass balance, J. Glaciol., 35, 355–369, 1989.
Jones, P. D., Jonsson, T., and Wheeler, D.: Extension to the North Atlantic Oscillation using early instrumental pressure observations from Gibraltar and South-West Iceland, Int. J. Climatol., 17, 1433–1450, 1997.
Laumann, T. and Reeh, N.: Sensitivity to climate change or the mass balance of glaciers in southern Norway, J. Glaciol., 39, 656–665, 1993.
Lliboutry, L.: Multivariate statistical analysis of glacier annual balances, J. Glaciol., 13, 371–392, 1974.
Maisch, M.: The long-term signal of climate change in the Swiss Alps: Glacier retreat since the end of the Little Ice Age and future ice decay scenarios, Geogr. Fis. Din. Quat., 23, 139–151, 2000.

Marzeion, B. and Nesje, A.: Spatial patterns of North Atlantic Oscillation influence on mass balance variability of European Glaciers, The Cryosphere Discuss., 6, 1–35, doi:10.5194/tcd-6-1-2012, 2012.

McCabe, G. J. and Wolock, D. M.: Long-term variability in Northern Hemisphere snow cover and associations with warmer winters, Climatic Change, 99, 141–153, 2010.

Müller, H. and Kappenberger, G.: Claridenfirn-Messungen 1914–1984, Zürcher Geogr. Schr., 40, 1991.

Oerlemans, J.: A model for the surface balance of ice masses: Part 1. Alpine glaciers, Z. Gletscherkd. Glazialgeol., 27–28, 63–83, 1993.

Oerlemans, J.: Glacier and Climate Change, A. A. Balkema, Lisse, The Netherlands, 148 pp., 2001.

Oerlemans, J. and Fortuin, J. P. F.: Sensitivity of glaciers and small ice caps to greenhouse warming, Science, 258, 115–117, 1992.

Oerlemans, J. and Hoogendoorn, N. C.: Mass-balance gradients and climate change, J. Glaciol., 35, 399–405, 1989.

Oerlemans, J., Anderson, B., Hubbard, A, Huybrechts, P., Jóhannesson, T., Knap, W. H., Schmeits, M., Stroeven, A. P., van de Wal, R. S. W., Wallinga, J., and Zuo, Z.: Modelling the response of glaciers to climate warming, Clim. Dynam., 14, 267–274, 1998.

Ohmura, A., Bauder, A., Müller, H., and Kappenberger, G.: Long-term change of mass balance and the role of radiation, Ann. Glaciol., 46, 367–374, 2007.

Osborn, T. J.: Recent variations in the winter North Atlantic Oscillation, Weather, 61, 353–355, 2006.

Pellicciotti, F., Helbing, J., Rivera, A., Favier, V., Corripio, J., Araos, J., Sicart, J. E., and Carenzo, M.: A study of the energy balance and melt regime on Juncal Norte Glacier, semi-arid Andes of central Chile, using melt models of different complexity, Hydrol. Process., 22, 3980–3997, 2008.

Perreault, L., Bernier, J., Bobée, B., and Parent, E.: Bayesian change-point analysis in hydrometeorological time series, Part 1, The normal model revisited, J. Hydrol., 235, 221–241, 2000a.

Perreault, L., Bernier, J., Bobée, B., and Parent, E.: Bayesian change-point analysis in hydrometeorological time series, Part 2, Comparison of change-point models and forecasting, J. Hydrol., 235, 242–263, 2000b.

Quadrelli, R., Lazzeri, M., Cacciamani, C., and Tibaldi, S.: Observed winter Alpine precipitation variability and links with large-scale circulation patterns, Clim. Res., 17, 275–284, 2001.

Rabatel, A., Dedieu, J. P., Thibert, E., Letréguilly, A., and Vincent C.: 25 years (1981–2005) of equilibrium-line altitude and mass-balance reconstruction on Glacier Blanc, French Alps, using remote-sensing methods and meteorological data, J. Glaciol., 54, 307–314, 2008.

Rasmussen, L. A.: South Cascade Glacier mass balance, 1935–2006, Ann. Glaciol., 50, 215–220, 2009.

Rasmussen, L. A. and Andreassen, L. M.: Seasonal mass balance gradients in Norway, J. Glaciol., 51, 601–606, 2005.

Scherrer, S. C. and Appenzeller, C.: Swiss Alpine snow pack variability: major patterns and links to local climate and large scale flow, Clim. Res., 32, 187–199, 2006.

Sicart, J. E., Hock, R., and Six, D.: Glacier melt, air temperature and energy balance in different climates: The Bolivian Tropics, the French Alps, and northern Sweden, J. Geophys. Res., 113, D24113, doi:10.1029/2008JD010406, 2008.

Six, D., Reynaud, L., and Letréguilly, A.: Alpine and Scandinavian glaciers mass balances, their relations with the North Atlantic Oscillation, Comptes Rendus de l'Académie des Sciences – Series IIA – Earth and Planetary Science, 333, 693–698, 2001.

Tanner, M. H.: Methods for the Exploration of Posterior Distributions and Likelihood Functions, Springer-Verlag, Berlin, 220 pp., 1996.

Thibert, E. and Vincent, C.: Best possible estimation of mass balance combining glaciological and geodetic methods, Ann. Glaciol., 50, 112–118, 2009.

Thibert, E., Blanc, R., Vincent, C., and Eckert, N.: Glaciological and volumetric mass balance measurements: Error analysis over 51 years for Glacier de Sarennes, French Alps, J. Glaciol., 54, 522–532, 2008.

Wallinga, J. and van de Wal, R. S. W.: Sensitivity of Rhonegletscher, Switzerland, to climate change: experiments with a one-dimensional flowline model, J. Glaciol., 44, 383–393, 1998.

Vallon, M., Vincent, C., and Reynaud, L.: Altitudinal gradient of mass-balance sensitivity to climatic change from 18 years of observations on Glacier d'Argentière, France, J. Glaciol., 44, 93–96, 1998.

van Loon, H. and Williams, J.: The connection between trends of mean temperature and circulation at the surface, Part I: Winter, Mon. Weather Rev., 104, 365–380, 1976.

Vincent, C.: Influence of climate change over the 20th century on four French glacier mass balances, J. Geophys. Res., 107, 4375, doi:10.1029/2001JD000832, 2002.

Vincent, C. and Vallon, M.: Meteorological controls on a glacier mass balance: empirical relations suggested by measurements on glacier de Sarennes, France, J. Glaciol., 43, 131–137, 1997.
Vincent, C., Kappenberger, G., Valla, F., Bauder, A., Funk, M., and Le Meur, E.: Ice ablation as evidence of climate change in the Alps over the 20th century, J. Geophys. Res., 109, D10104, doi:10.1029/2003JD003857, 2004.
Zemp, M., Hoelzle, M., and Haeberli, W.: Distributed modelling of the regional climatic equilibrium line altitude of glaciers in the European Alps, Global Planet. Change, 56, 83–100, 2007.

Table 1. Time structure identified by the analysis of variance in the seasonal components of the balance: time change τ, means and trends in subsequent periods (Eckert et al., 2011).

	change point, τ	**mean** (m w.e. yr^{-1}) trend (cm w.e. yr^{-2})		
		1949–1976	1977–2007	
winter balance	1976	**1.48** −1.3	**1.88** −0.7	
		1949–1982	1983–2007	
summer balance	1982	**−2.26** +2.4	**−3.22** −1.5	
		1949–1976	1977–1982	1983–2007
annual balance	1976–1982	**−0.80** +1.1	**0** +1.7	**−1.36** −2.2

TCD
6, 2115–2160, 2012

Table 2. Correlation matrix between the different time series. Bold face values are significant non zero correlations at the 95 % confidence level.

Variables	Annual balance	Summer balance	Winter balance	Besse precipitation	Lyon temperature	DJF NAO	NDJFMA NAO	Annual NAO
Annual balance	**1**	**0.89**	**0.53**	**0.6**	**−0.64**	−0.25	−0.25	−0.1
Summer balance		**1**	0.08	**0.27**	**−0.76**	**−0.33**	**−0.32**	−0.11
Winter balance			**1**	**0.81**	0.02	0.08	0.06	−0.02
Besse precipitation				**1**	−0.08	−0.03	−0.03	−0.03
Lyon temperature					**1**	**0.41**	**0.37**	0.02
DJF NAO						**1**	**0.93**	**0.67**
NDJFMA NAO							**1**	**0.75**
Annual NAO								1

Discussion Paper | Discussion Paper | Discussion Paper | Discussion Paper |

TCD

6, 2115–2160, 2012

An analysis of 6 decades at Glacier de Sarennes

E. Thibert et al.

Table 3. Correlation matrix between trends in the different time series. Bold face values are significant non zero correlations at the 95 % confidence level. All trends are provided by the variance decomposition model of Eq. (2), apart from trends in NAO anomalies resulting from the 7-year triangular moving averages.

Variables	Annual balance	Summer balance	Winter balance	Besse precipitation	Lyon temperature	DJF NAO	NDJFMA NAO	Annual NAO
Annual balance	**1**	**0.91**	−0.21	**0.32**	**−0.84**	**−0.44**	**−0.39**	0.05
Summer balance		**1**	**−0.59**	−0.08	**−0.94**	**−0.57**	**−0.51**	−0.04
Winter balance			**1**	**0.81**	**0.59**	**0.50**	**0.45**	0.20
Besse precipitation				**1**	0.02	**0.35**	**0.28**	**0.33**
Lyon temperature					**1**	**0.45**	**0.42**	−0.09
DJF NAO						**1**	**0.93**	**0.67**
NDJFMA NAO							**1**	**0.75**
Annual NAO								**1**

Table 4. Amount, duration and rate for indistinct snow and ice ablations at Sarennes over whole period of record and before and after the change point identified by the analysis of variance. Bold face values are variations after the 1982 change point identified in the summer balance time series.

	Total ablation (snow and ice)		
	mean ($m\,w.e.\,yr^{-1}$)	duration (days)	rate ($cm\,w.e.\,day^{-1}$)
1949–2007	2.55	125	2.03
1949–1982	2.08	115	1.84
1983–2007	3.18	139	2.28
	(+1.10)	**(+24)**	**(+0.44)**

TCD
6, 2115–2160, 2012

Table 5. Amount, duration and rate for snow and ice ablation at Sarennes over whole period of record as well as before and after the change point identified by the analysis of variance. Bold face values are differences after the 1982 change point identified in the summer balance time series.

	Snow ablation			Ice ablation		
	mean ($\mathrm{m\ w.e.\ yr^{-1}}$)	duration (days)	rate ($\mathrm{cm\ w.e.\ day^{-1}}$)	mean ($\mathrm{m\ w.e.\ yr^{-1}}$)	duration (days)	rate ($\mathrm{cm\ w.e.\ day^{-1}}$)
1949–2007	1.54	86	1.88	1.01	39	2.59
1949–1982	1.42	86	1.77	1.07	29	2.50
1983–2007	1.70	86	2.04	1.80	53	2.75
	(+0.28)	**(0)**	**(+0.27)**	**(+0.73)**	**(+24)**	**(+0.25)**

TCD
6, 2115–2160, 2012

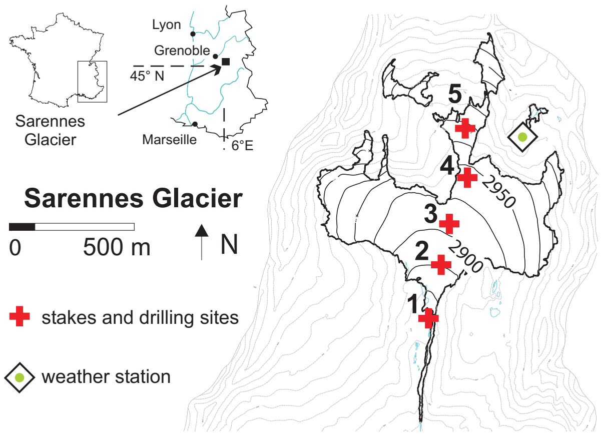

Fig. 1. Location of stakes where balance is measured at Sarennes Glacier. Contour lines on the glacier are at 25 m intervals.

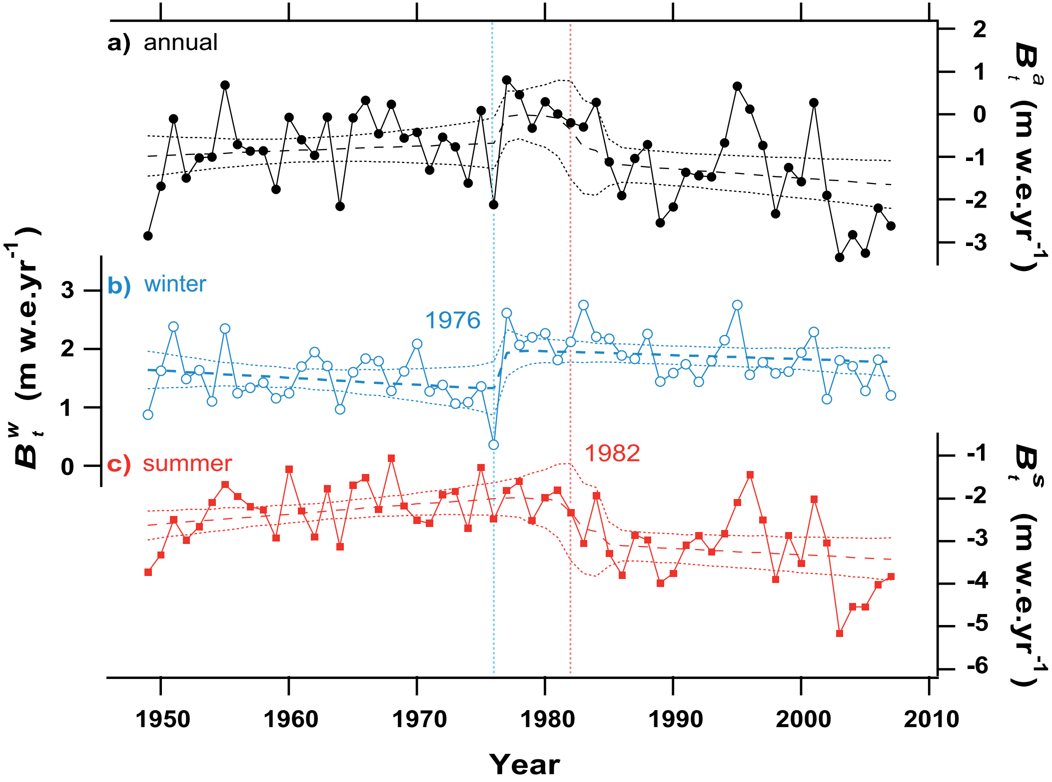

Fig. 2. (a) Annual, **(b)** winter, and **(c)** summer glacier-wide balances at Sarennes extracted from the analysis of variance. Dashed lines are trends and dotted lines are 95 % credible intervals for the trends. The blue and red vertical dotted lines highlight the change points in winter and summer balances in 1976 and 1982, respectively.

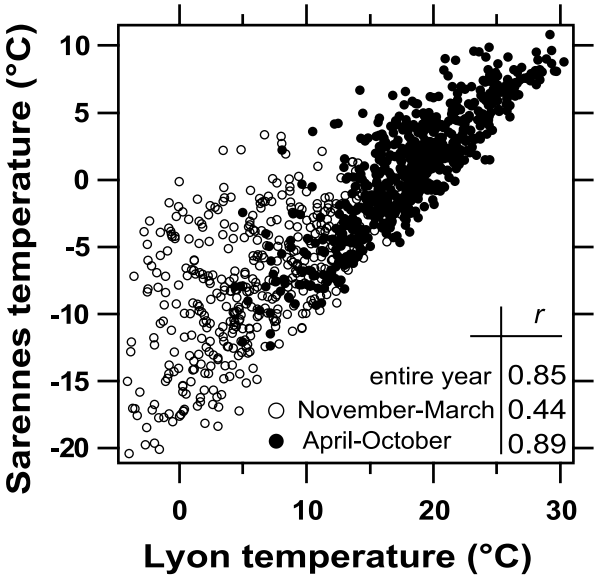

Fig. 3. Correlation between daily temperatures measured at Sarennes (3070 m) and Lyon-Bron (200 m a.s.l.) recorded over 2004–2007.

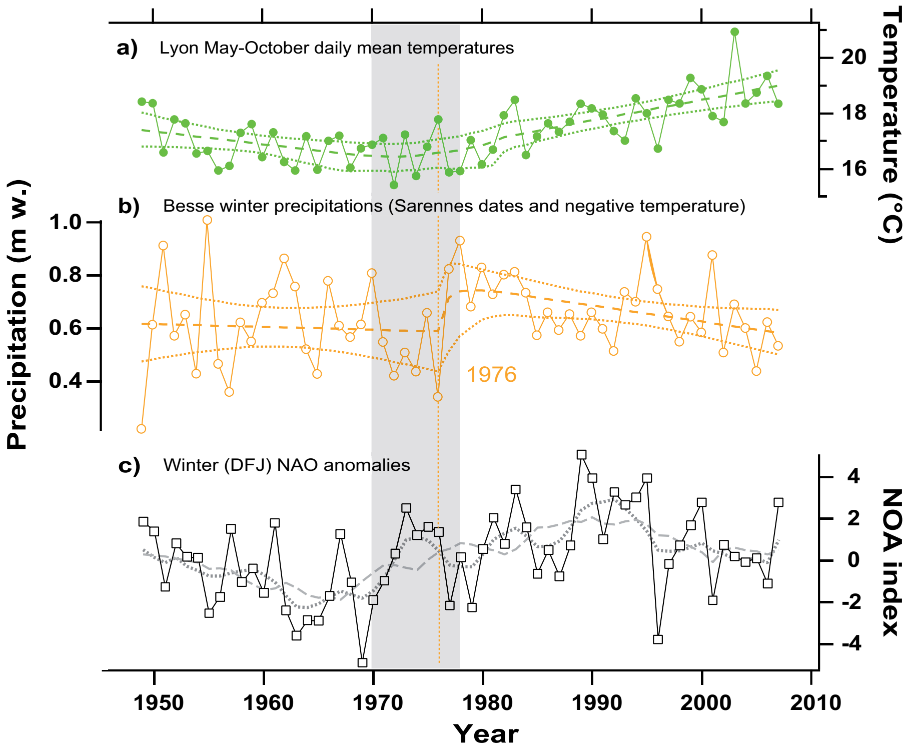

Fig. 4. (a) May to October daily mean temperatures at Lyon-Bron (200 m a.s.l.) weather station with trends (dashed line) and 95 % credible intervals (dotted line) for the trends; **(b)** winter precipitation amount recorded at Besse (1400 m a.s.l.) weather station according to Sarennes measurement dates and negative temperature on the glacier, with trends (dashed line) and 95 % credible intervals (dotted line) for the trends; **(c)** December to January (DFJ) NAO anomalies (black line and squares), 5-yr smoothed data (grey dotted line), 11-yr smoothed (grey dashed line). The time range in grey is the gradual change point (1974 ± 4 yr) in the temperature signal.

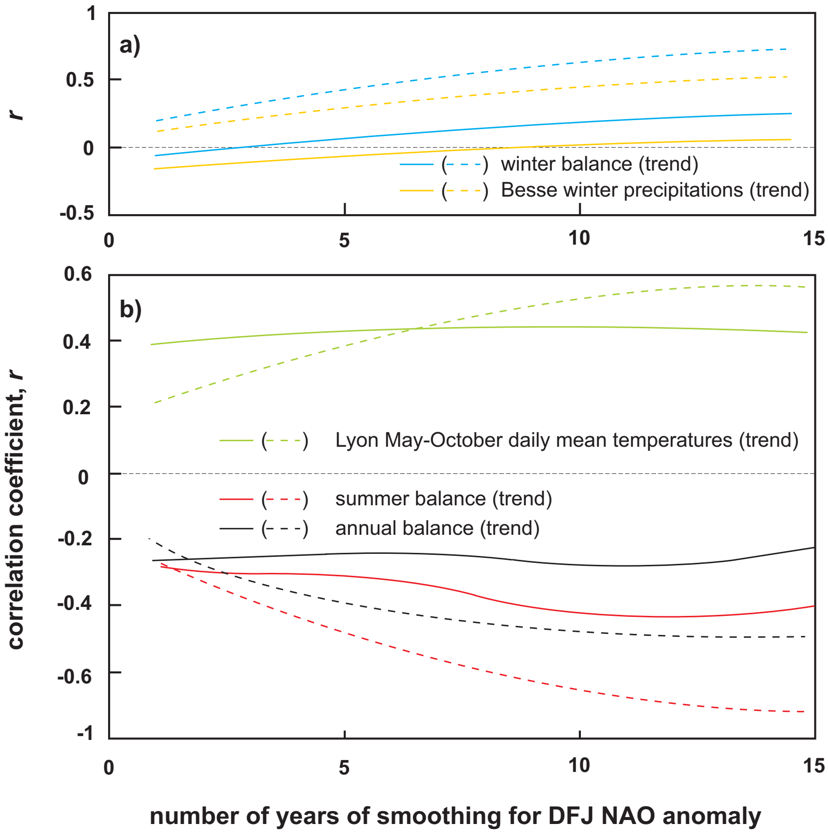

Fig. 5. Correlation between NAO winter (DFJ) anomalies and local variables as a function of the level of smoothing. **(a)** Winter variables: winter mass-balance and Besse winter precipitations); **(b)** summer/annual variables: summer and annual mass-balances, and Lyon-Bron May to October mean temperatures. Continuous and dashed line refer to annual and trends of local variables, respectively.

TCD
6, 2115–2160, 2012
An analysis of 6 decades at Glacier de Sarennes
E. Thibert et al.

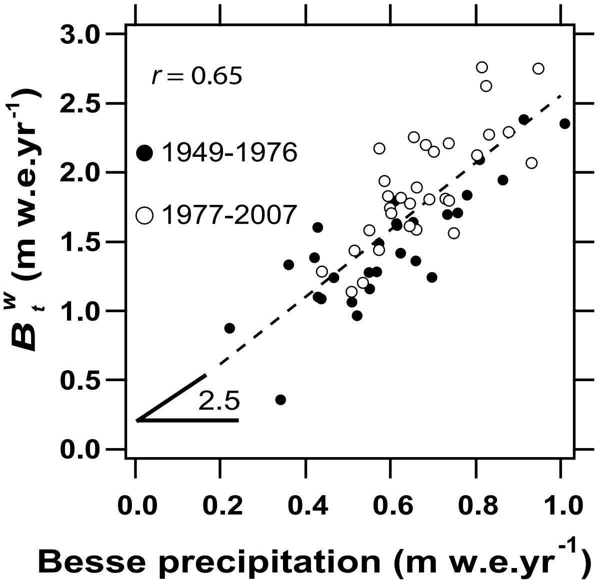

Fig. 6. Glacier-wide winter balance at Sarennes as a function of precipitation recorded at Besse weather station (for only days with precipitation and a temperature of below 0 °C at Sarennes).

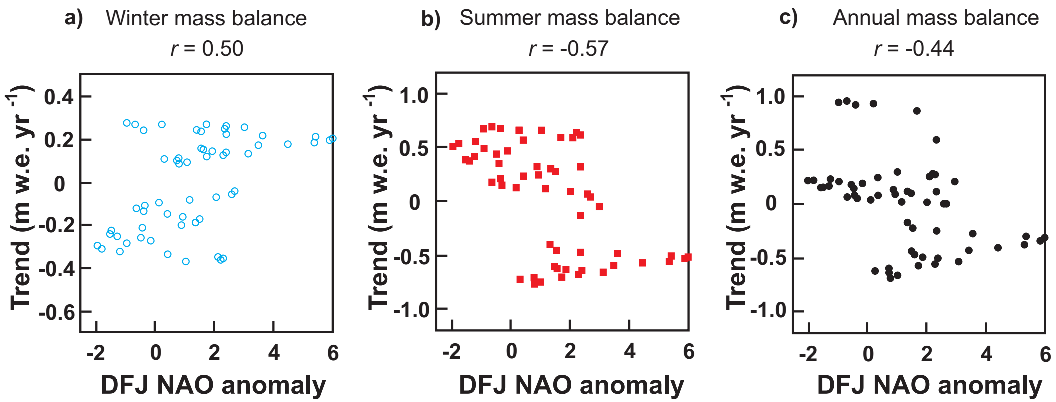

Fig. 7. Correlation between NAO anomalies (7-yr smoothed DFJ) and the three components of Sarennes winter **(a)**, summer **(b)** and annual **(c)** mass-balance trends provided by the variance analysis.

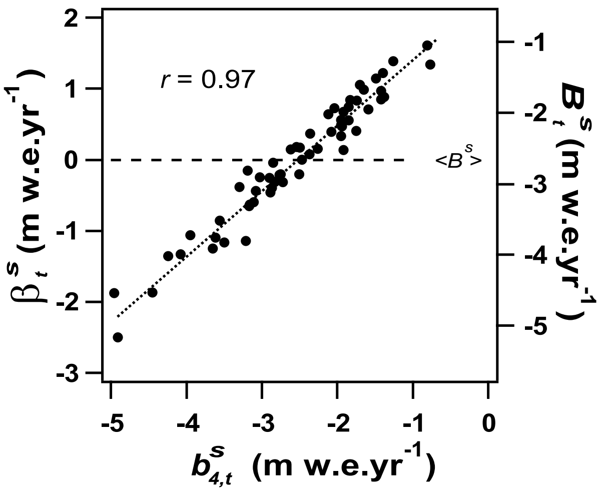

Fig. 8. Selection of a single stake to represent the overall summer centred balance, β_t^s or glacier-wide summer balance B_t^s. Stake 4 is the best estimator and the summer balance, $b_{4,t}^s$, recorded at this location is highly correlated to the centred summer balance.

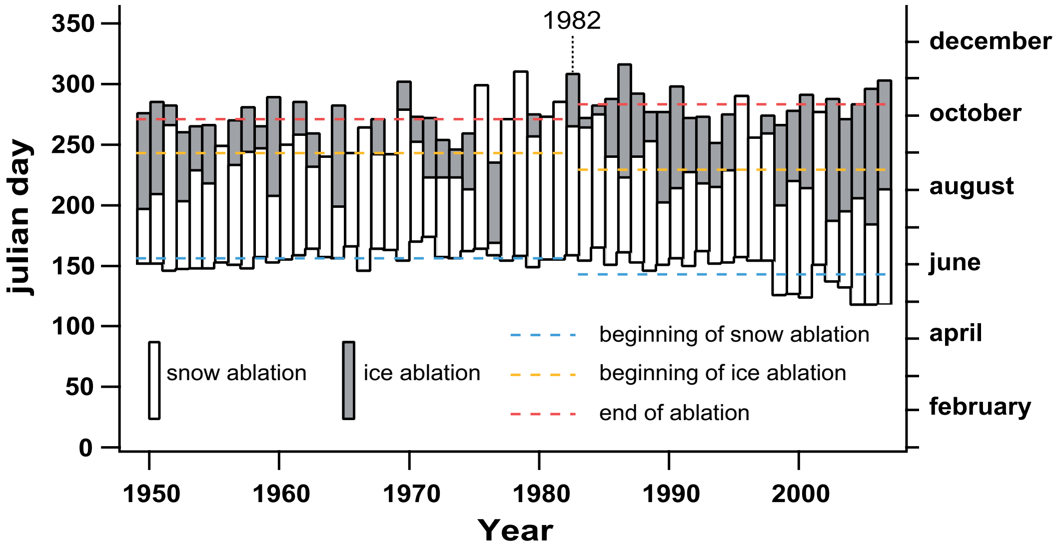

Fig. 9. Ablation start, end and duration for snow and ice at stake 4 over the 6 decades at Sarennes. In dashed line are mean values before and after the change point identified in 1982 for the summer balance.

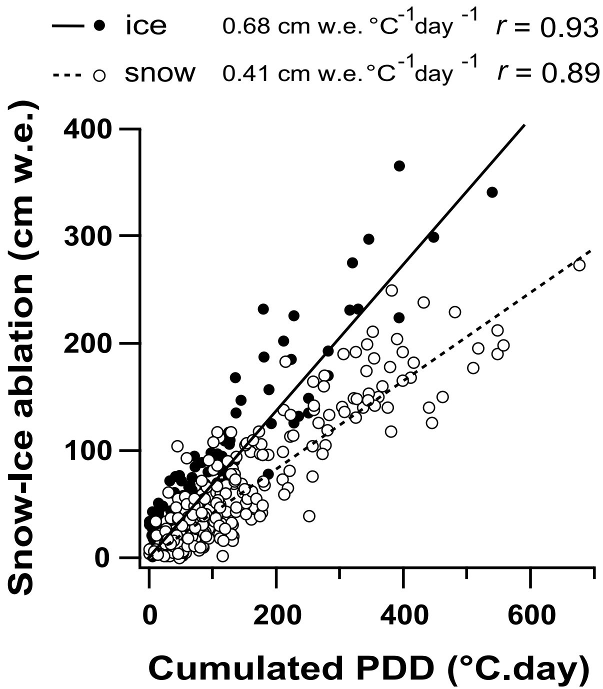

Fig. 10. Measured ablation at stake 4 for snow and ice as function of the cumulated positive degree-day calculated from Lyon with a vertical lapse rate of 6.25° C km^{-1}.

TCD
6, 2115–2160, 2012

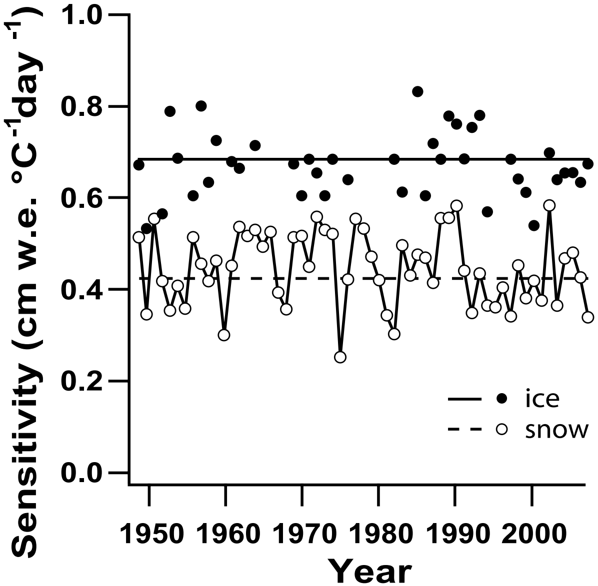

Fig. 11. Sensitivity of snow and ice ablation to positive temperatures along the 6 decades at Sarennes at stake 4. Ice ablation has occurred on 41 yr among the 59 yr of the record.

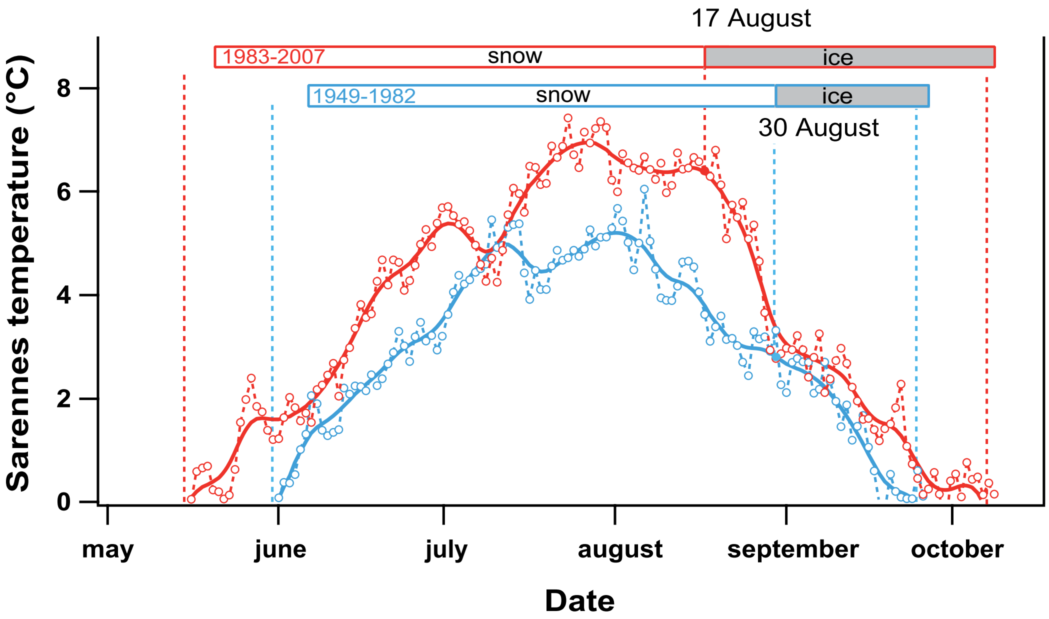

Fig. 12. Mean daily temperature above 0° C at Sarennes (3000 m) between 1949–1982 (blue curve) and 1983–2007 (red curve) explaining the lengthening of the ablation season with earlier snow melt in May, earlier ice melt in August and later ice melt in October according to the PDD model. Dashed lines and markers are raw daily means while continuous lines are Gaussian smoothed daily means. Horizontal bars are observed average ablation durations at stake 4 for snow (white) and ice (grey) for the 2 periods.

TCD
6, 2115–2160, 2012